

# Studies on the Adsorption of 2-Chlorophenol onto Rice Straw Activated Carbon from Aqueous Solution and its Regeneration



This work is licensed under a Creative Commons Attribution 4.0 International License

M. K. Mahapatra\* and A. Kumar

Department of Chemical Engineering,  
National Institute of Technology,  
Rourkela -769008, Odisha, India

doi: <https://doi.org/10.15255/CABEQ.2021.2004>

Original scientific paper  
Received: August 13, 2021  
Accepted: March 2, 2022

For this study a low-cost adsorbent, rice straw activated carbon (RSAC) was prepared via thermochemical routes after being impregnated with  $ZnCl_2$ . Characterization studies performed on RSAC have revealed that RSAC is a mesoporous adsorbent with significant affinity towards 2-chlorophenol (2-CP). The optimal values for process parameters were investigated via experimental runs. The optimal values of process parameters such as RSAC dose, pH of 2-CP solution, contact time, and temperature were found to be;  $1.25 \text{ g L}^{-1}$ , 8, 125 min, and 303 K, respectively. The Langmuir isotherm and pseudo-first-order kinetics models were found to be in good agreement with the experimental data for this adsorption system. The adsorption thermodynamics studies have revealed that the adsorption of 2-CP onto RSAC is exothermic and spontaneous. Regeneration studies of RSAC using hydrogen peroxide have revealed that RSAC was effectively regenerated for four consecutive cycles. This research has proved the potential of RSAC for abating 2-CP from aqueous solutions.

## Keywords:

adsorption, 2-chlorophenol abatement, rice straw activated carbon, adsorption kinetics, adsorption equilibrium, regeneration

## Introduction

Pollution has a devastating effect on every subdivision of the ecosystem. In the current era, the absolute necessities for the human race like dyes and paints, medicines, various pesticides, germicides, defoliants, disinfectants, etc., have become harmful for the ecosystem. Among pollutants, halogenated aromatic compounds are highly stable. Halogenated aromatics have carcinogenic and mutagenic properties and can cause incurable diseases.<sup>1</sup>

2-Chlorophenol (2-CP) is a halogenated aromatic compound and has been proactively used in many industrial sectors such as pesticides, polymer, pharma, petroleum, assorted chemicals, etc.<sup>2</sup> United States Environmental Protection Agency (USEPA) has classified 2-CP as a priority organic pollutant and enacted a permissible limit of 0.1 ppb for drinking water.<sup>3</sup> 2-CP makes its way into the ecosystem via industrial effluents, agricultural run-offs, and leachates from contaminated places and landfills.<sup>4</sup> 2-CP has the tendency to biomagnify owing to its poor biodegradability. As a potent mutagenic and carcinogenic agent, 2-CP has devastating effects on the aquatic ecosystem.<sup>5</sup> Hence, the abatement of

2-CP is an essential activity in environmental protection.

Diverse methods have been deployed to abate 2-CP from wastewater like chemically induced precipitation, reverse osmosis (RO), oxidation-reduction, and adsorption.<sup>6–8</sup> Among these techniques, adsorption has evolved as the most reported technique owing to its cost-effectiveness and high efficiency in effluent treatment. The quest for the development of cheaper adsorbents as the replacement for costly synthetic adsorbents has escalated in recent years. Adsorbents prepared from waste biomasses are gaining attention as potential adsorbents for removing hazardous pollutants, including 2-CP.<sup>8,9</sup>

Several researchers have studied activated carbon prepared from rice straw (RS). However, in this research, the RSAC was prepared using  $ZnCl_2$ , and applied for the abatement of 2-CP. Moreover, there is no literature supporting both cases, i.e., RSAC preparation as per the protocol reported here and its application for 2-CP abatement, which is the novelty of this research.

The advantage of RSAC over other adsorbents comes from its three distinctive features; cost-effective adsorbent, rejuvenation ability, and alternative fuel usability potential. Rice straw is a renewable

\*Corresponding author: Tel.: +91 7540946964; fax: +91 661 2472999.  
E-mail address: [manojmahapatra2010@gmail.com](mailto:manojmahapatra2010@gmail.com)

agricultural biomass and is widely available. It can be purchased at very low prices, making the whole adsorption process cheaper by preparing cost-effective adsorbents. The rejuvenation study in this research has proven the reusability potential of RSAC. The reusability potential will reduce the cost of the wastewater treatment process. Elemental analysis studies have confirmed the abundance of carbon content in RSAC, thus making it a potential candidate for afterlife usage as a solid fuel alternative to coal.<sup>10</sup>

This study carried out the detailed procedure of RSAC preparation and its characterization. Parameter optimization was carried out for achieving the highest abatement on pH, adsorbent dose, adsorbate-adsorbent contact time, adsorbate concentration, and adsorption system temperature. The experimental data were modeled with various models pertaining to adsorption equilibrium, kinetics, and thermodynamics in order to enunciate the characteristic of 2-CP adsorption onto the RSAC. The regeneration potential of RSAC was also evaluated.

## Materials and methods

### Rice straw activated carbon (RSAC) preparation

The decisive criteria such as low cost, higher carbon content, and abundance play a crucial role in finalizing any potential raw material for activated carbon preparation.<sup>8,11</sup> In this research work, a cheaper adsorbent from rice straw was prepared in the laboratory, and then subjected to the evaluation of 2-CP adsorption capabilities. The rice straw was procured from the local farmers near Rourkela city. The rice straw was then thoroughly washed under tap water to remove dirt and soil. The rice straw was then thoroughly dried using a hot air oven, and subsequently, the dried rice straw was chopped into about 1-cm long strands to make the further processing steps easier. The rice straw was then subjected to chemical activation by agitation with CaO, ZnCl<sub>2</sub>, and RS in the (w/w) percentage ratio of 12 %, 36 %, and 52 %, respectively, along with distilled water for 50 min. After chemical treatment, the rice straw was dried and subsequently carbonized in a muffle furnace at the activation temperature of 623 K for 1 h in an inert environment. The respective values reported for impregnation ratio, impregnation time, and activation temperatures have resulted in the highest yield of RSAC (detailed optimization study of RSAC preparation has been communicated elsewhere for publication). Liang *et al.* reported a similar analysis of activated carbon (AC) preparation based on impregnation ratio, activation temperature, and AC yield.<sup>12</sup>

The resultant RSAC was then washed with 10 % HCl solution to remove Zn. Subsequently, the RSAC was powdered using a mixer grinder, and the powdered RSAC was sieved using mesh number 30. The sieved RSAC was washed thoroughly with deionized double distilled water until the supernatant returned neutral pH. Following washing, the RSAC was oven-dried at 353 K for 20 h and then stored in airtight containers until further application. The schematic representation of RSAC preparation is presented in Fig. 1.

### Characterization of RSAC

The composition analysis of RSAC was carried out by proximate, ultimate, and EDX analyses. Proximate analysis was done to determine the weight percentages of moisture (ASTM D2867 – 09), volatile matter (ASTM D5832 – 98), ash (ASTM D2866 – 94), fixed carbon content (differential) using standard protocols. Egboosiuba *et al.* reported the usage of standard protocols for the proximate analysis. The fixed carbon content was determined by using Eq. 1. The elemental composition analysis for carbon, hydrogen, nitrogen, and sulfur was determined the ultimate analysis using a CHNS analyzer (Elementar Vario EL III, Germany). The oxygen composition was evaluated using Eq. 2.<sup>13</sup> The EDX analysis was carried out using an energy dispersive X-ray analyzer coupled with a scanning electron microscope (JSM-6480LV, JEOL, Japan).

$$\text{FC}(\text{wt}\%) = [100 - (\text{MC}(\text{wt}\%) + \text{VM}(\text{wt}\%) + \text{Ash}(\text{wt}\%))] \quad (1)$$

$$\text{Oxygen}(\text{wt}\%) = [100 - (\text{carbon}(\text{wt}\%) + \text{nitrogen}(\text{wt}\%) + \text{hydrogen}(\text{wt}\%) + \text{sulfur}(\text{wt}\%))] \quad (2)$$

Adsorbent surface charge determination is an essential characterization study since; it helps in understanding the adsorption mechanism. In this study, the salt addition method was employed to analyze the surface charge of RSAC, including the point of zero charge (pH<sub>pzc</sub>) following the protocol reported by Mahmood *et al.* The pH values in this analysis were measured using a pH meter (μ pH system 361, Systronics, India). The plot between ΔpH against pH<sub>i</sub> gives the value of the pH<sub>pzc</sub> (where the curve bisects the x-axis).<sup>14</sup>

The functional groups on the RSAC surface were detected via Fourier-transform infrared (FTIR) analysis in attenuated total reflection (ATR) mode using the FTIR analyzer (Bruker α alpha-E, USA). The surface morphology of RSAC was analyzed using a scanning electron microscope (JSM-6480LV, JEOL, Japan). The surface area of the RSAC, pore-volume, and pore diameters were evaluated by Brunauer-Emmett-Teller (BET) analysis (TriStar

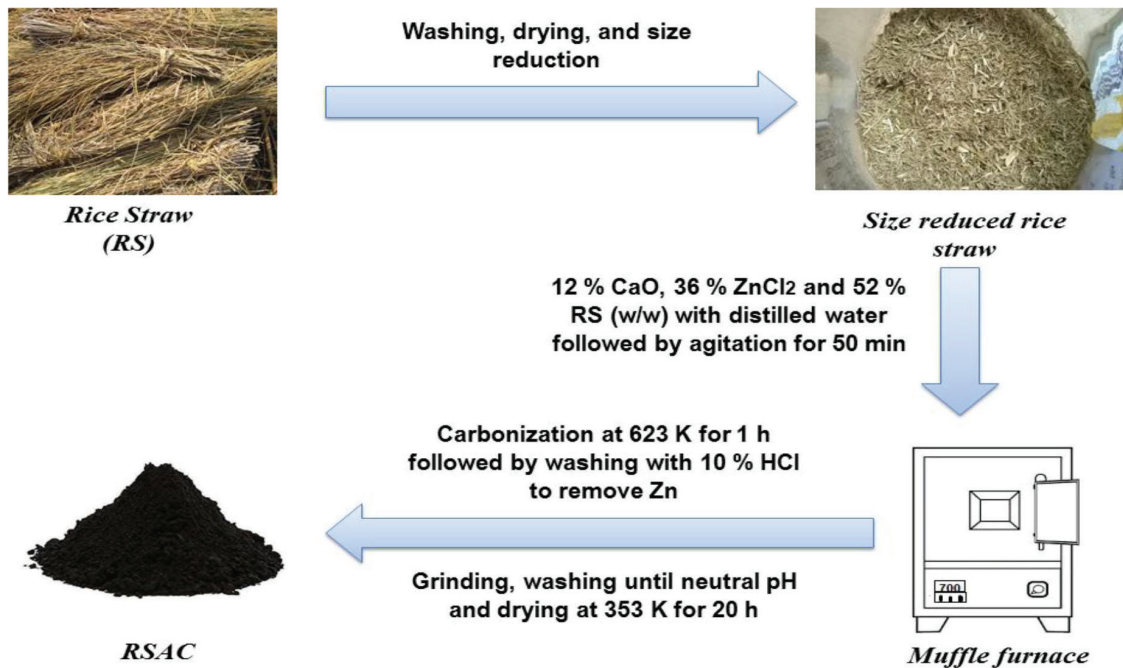


Fig. 1 – Schematic representation of RSAC synthesis

3000, Micromeritics Instrumentation Corporation, USA). Table 1 presents the results of the aforementioned analyses.

#### Adsorbate

The synthetic stock solution of 2-CP at an initial concentration of 500 mg L<sup>-1</sup> was prepared by dissolving the requisite amount of 2-CP in deionized double-distilled water. Experimental samples with appropriate concentrations were made from the stock solution by appropriate dilution. The pH of the sample solutions was maintained using 0.1 N HCl and 0.1 N NaOH as per need. The 2-CP (purity 97 %) was of analytical grade and procured from Loba Chemie, India. The analytical grade inorganic chemicals were procured from Fisher Scientific, India.

#### Batch adsorption experiments

For the batch adsorption studies, 50 mL of 2-CP of requisite concentration at desired pH were placed in 150-mL screw-capped conical flasks along with an appropriate amount of the RSAC. This entire setup was allowed for thorough agitation using an incubator shaker (Naanolab, India) at 120 rpm. After the experimental run, three-milliliter supernatant was sampled for each sampling. The supernatant was then subjected to centrifugation at 7000 rpm for 10 min in a temperature-controlled centrifuge (Biotechnologies Inc., India) for separating adsorbent particles. The centrifuged samples were then analyzed using a UV-Vis spectrophotometer. The 2-CP adsorption efficiency and capacities of RSAC

were evaluated by calculating removal percentage and equilibrium uptake capacities, using equations 3 and 4, respectively.

$$\text{Removal percentage, \%R} = 100 \left( \frac{X_0 - X_t}{X_0} \right) \quad (3)$$

where  $X_0$  (mg L<sup>-1</sup>) = 2-CP concentration before adsorption

$X_t$  (mg L<sup>-1</sup>) = 2-CP concentration after adsorption at time  $t$ .

The adsorption capacity of RSAC was estimated using Eq. 4:

$$\text{Adsorption capacity, } q_e = \frac{(X_0 - X_e)V}{w} \quad (4)$$

where  $q_e$  (mg g<sup>-1</sup>) is the quantity of 2-CP adsorbed by RSAC at equilibrium,  $X_0$  and  $X_e$  (mg L<sup>-1</sup>) are 2-CP concentrations before adsorption and at equilibrium, respectively.

$V$  (L) is the initial volume of 2-CP.

$w$  (g) is the amount of RSAC.

Following this procedure, the optimal conditions for several factors affecting the adsorption of 2-CP, such as contact time, pH, 2-CP concentration, RSAC dose, and adsorption system temperatures, were evaluated. Subsequently, the adsorption equilibrium and kinetics studies were performed using the optimal conditions of the aforementioned parameters.

#### Analysis methodology

The remnants of 2-CP in the synthetic solution were evaluated via UV-Vis spectrophotometer (UV-

1800, Shimadzu, Japan) analysis. The samples were analyzed at the wavelength for the maximum absorbance of 2-CP, i.e.,  $\lambda_{\max} = 273$  nm. The standard calibration curve was plotted using the absorbance against the respective 2-CP concentration. The straight-line equation of the calibration plot was used to evaluate the unknown remnant values of 2-CP.

### Regeneration studies of RSAC

Adsorbent reusability aims to reduce the cost of 2-CP abatement operation and simultaneously enhance the efficiency of the adsorbent being used. In this research, the RSAC was regenerated by agitating the 2-CP loaded RSAC in eluents like 4 %

(v/v) hydrogen peroxide ( $H_2O_2$ ) solution at 305 K for 90 min followed by 7 % (w/v) NaOH solution at 318 K for 50 min. After treatment with eluents, the adsorbents were collected by filtration. Subsequently, they were subjected to thorough washing and drying, and reused for further adsorption runs. Mahapatra and Kumar, used a similar approach to regenerate neem seed activated carbons.<sup>15</sup>

## Results and discussion

### Characterization of RSAC

The composition of RSAC was analyzed via proximate and ultimate analyses, and the results are given in Table 1. The surface charge analysis studies revealed that the RSAC surface had  $pH_{pzc} = 7.5$  represented by Fig. 2(a), implying that below and beyond this value the surface will be positively and negatively charged, respectively.

Table 1 – Characterization of RSAC

Proximate analysis	
Components	(wt%)
Fixed carbon content	56.33
Ash content	4.28
Moisture content	3.11
Volatile matter content	36.27
Ultimate analysis	
Components	(wt%)
Carbon	55.48
Hydrogen	6.78
Nitrogen	3.07
Sulfur	1.15
Oxygen	33.52
EDX analysis	
Components	(wt%)
Carbon	66.38
Oxygen	27.96
Potassium	0.69
Aluminium	0.83
Silicon	1.97
Chlorine	2.17
Point of zero charge ( $pH_{pzc}$ )	7.5
Surface area, pore volume, and pore diameter analysis	
Surface area of pores	( $m^2 g^{-1}$ )
Brunauer-Emmett-Teller	239
Barrett-Joyner-Halenda cumulative volume of pore	( $cm^3 g^{-1}$ )
Single point total	0.186
Average pore width	Å
Brunauer-Emmett-Teller	25.62

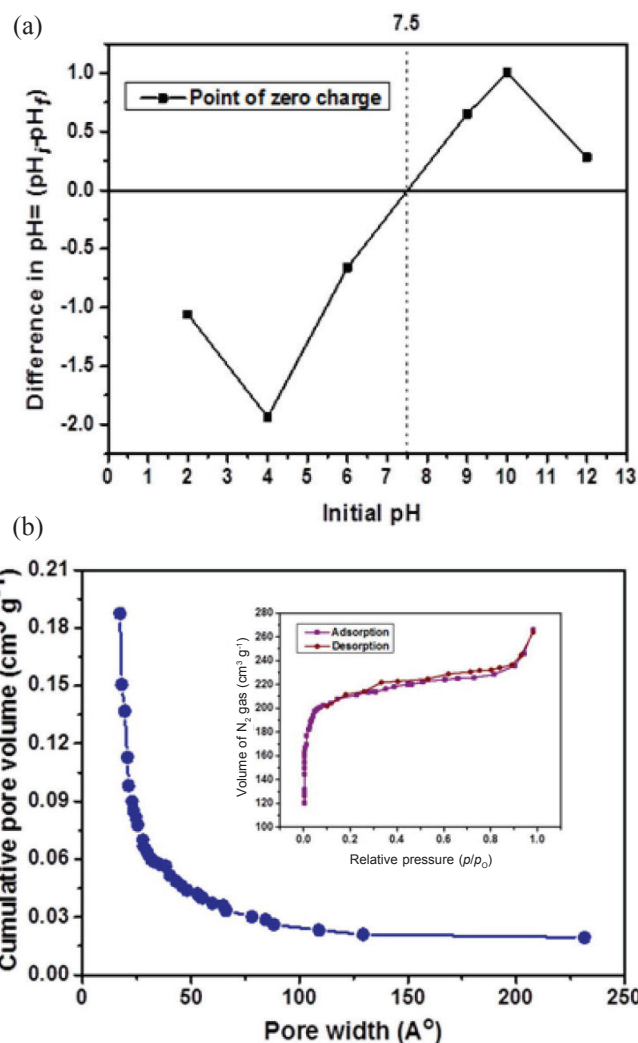


Fig. 2 – (a) Point of zero charge for RSAC, (b) BET hysteresis and pore characteristics of RSAC

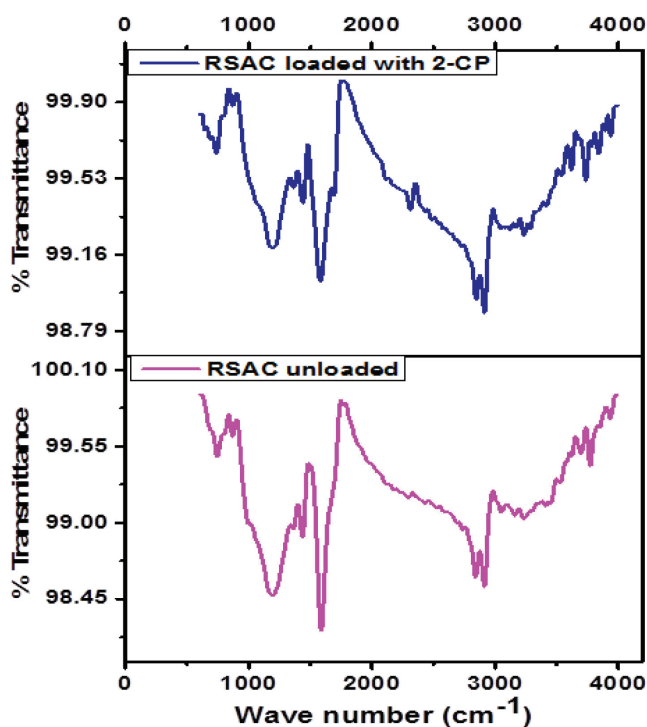


Fig. 3 – FTIR spectra of RSAC before and after adsorption of 2-CP

The surface area and pore properties of RSAC were investigated with the help of nitrogen adsorption and desorption cycles by the BET isotherm model. From Fig. 2(b), it can be concluded that the hysteresis profile has represented type-IV isotherm. The distinctive hysteresis loop has depicted the presence of mesopores in RSAC. Furthermore, it was observed that the inflection with the isotherm was in the range of 0.4–1.0 of the relative pressure ratio, which provides evidence for capillary condensation characteristics.<sup>16</sup> From BET analysis, the surface area, total pore volume, and average pore diameter were found to be 239 m<sup>2</sup> g<sup>-1</sup>, 0.186 cm<sup>3</sup> g<sup>-1</sup>, and 25.62 Å, respectively.

The FTIR spectra (Fig. 3) have revealed the characteristic vibrational frequencies of different functional groups present on the surface of RSAC. Alcoholic O–H bond stretching vibrations were found at 3173 and 3069 cm<sup>-1</sup>. Conjugated anhydride carbonyl (C=O) groups were found at 1730 cm<sup>-1</sup>. Stretching vibrations from sulfinyl S=O group, of sulfoxides, were observed at 1032 cm<sup>-1</sup>. Hydroxyl groups (O–H) with bending vibrations from phenolic compounds were observed at 1373 cm<sup>-1</sup>. Carbonyl groups (O=C=O) with strong stretching vibrations depicting carbon dioxide were observed at 2324 and 2326 cm<sup>-1</sup>. Strong sulfinyl groups (S=O) were observed from sulfates at 1414 cm<sup>-1</sup>. Strong carbonyl groups (C=O) with stretching vibrations were observed at 1699 cm<sup>-1</sup> belonged to the conjugated aldehydes. Strong alkyl halide groups con-

taining chlorine atom (C–Cl) pertaining to the halogenated compounds were observed at 675 and 720 cm<sup>-1</sup>. Carbonyl groups (C=O) from conjugated acid halides were observed at 1797 cm<sup>-1</sup>.<sup>17–19</sup>

From the SEM and EDX micrographs presented in Fig. 4(a), 4(b), 4(c), and 4(d), it is evident that the surface of RSAC is full of very shallow cavities and hollow tubular structures. Moreover, inside those cavities and tubular structures were distinct pores with varying sizes that may have formed due to chemical impregnation and further high-temperature carbonization could be observed. The larger pores on RSAC collectively represented a net-like structural formation (Fig. 4(c)). The EDX analysis revealed that carbon and oxygen were predominantly present in the activated carbon along with aluminum, potassium, silicon, and chlorine in minor quantities. RSAC's high carbon content makes it a suitable candidate for chlorophenol adsorption.<sup>20</sup>

### Effect of various factors on adsorption studies

#### Effect of RSAC dose

For investigating the optimal dose of RSAC, the weight of RSAC was varied from 0.2 to 6 g per liter of 2-CP solution with an initial 2-CP concentration of 100 mg L<sup>-1</sup> (Fig. 5(a)). From the plot, it was observed that an increase in RSAC dose resulted in a decrease of 2-CP uptake capacity. On the contrary, the removal percentage has showed an increasing trend. The corresponding RSAC dose at the point of intersection of two curves mentioned above was considered the optimal value of the RSAC dose, which was 1.25 g L<sup>-1</sup>. A decrease in RSAC's uptake capacity was observed with a corresponding increase in dose owing to the absence of sufficient 2-CP species.<sup>21–23</sup>

#### Effect of adsorbate solution pH

The pH plays a crucial role in the entire 2-CP-RSAC adsorption process and significantly affects the adsorption capacity of RSAC. The experimental runs were made for different pH in the bracket of 2–12, keeping the other factors constant. From Fig. 5(b), it is evident that 2-CP adsorption capacity was favored by pH increment. At pH = 8, the highest uptake capacity of 22 mg g<sup>-1</sup> was observed. A further increase in pH followed a declining trend in 2-CP adsorption. The varying trend of pH-dependent adsorption capacity is supported by the concepts of the acid dissociation constant (pK<sub>a</sub>) of 2-CP. The pK<sub>a</sub> value of 2-CP is 8.56, meaning that when pH < pK<sub>a</sub>, the 2-CP remains neutral in the aqueous solution, but when pH > pK<sub>a</sub>, the 2-CP is found in anionic form as 2-chlorophenolate ions. The highest removal of 2-CP by RSAC was regis-

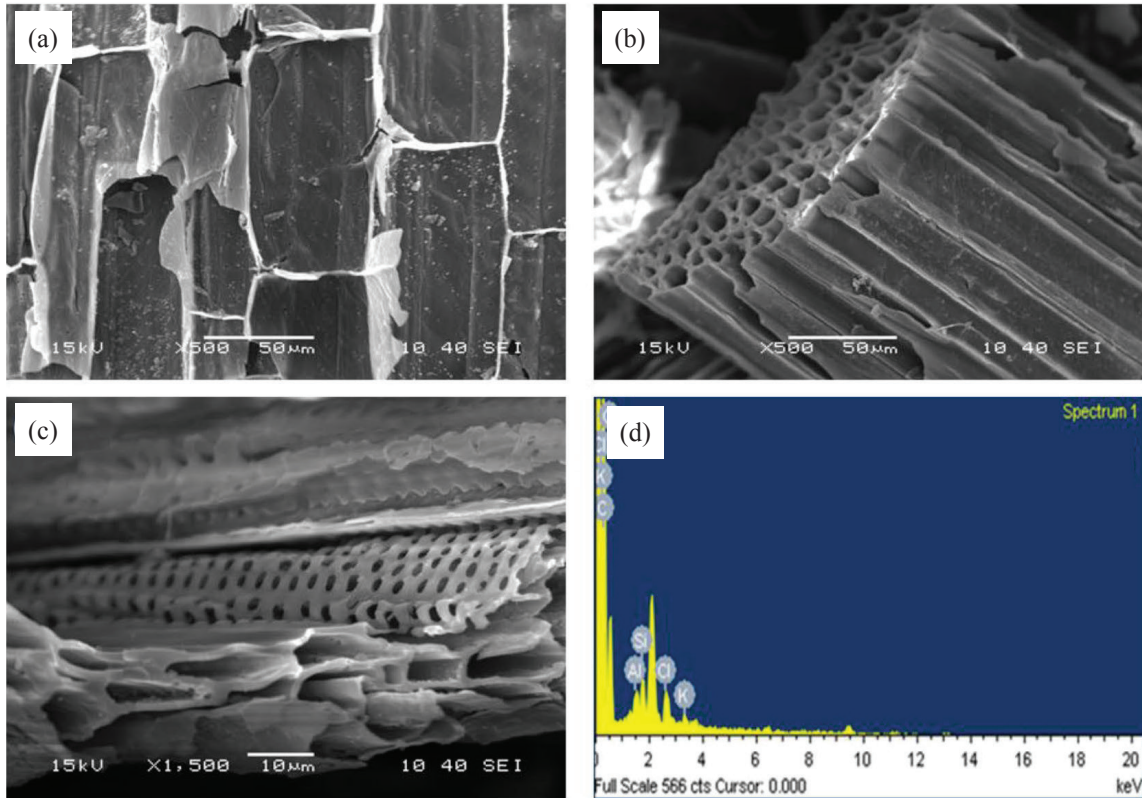


Fig. 4 – Micrographs of SEM analysis for RSAC (a) 500x magnification, (b) 500x magnification, (c) 1500x magnification, (d) EDX spectrum of RSAC

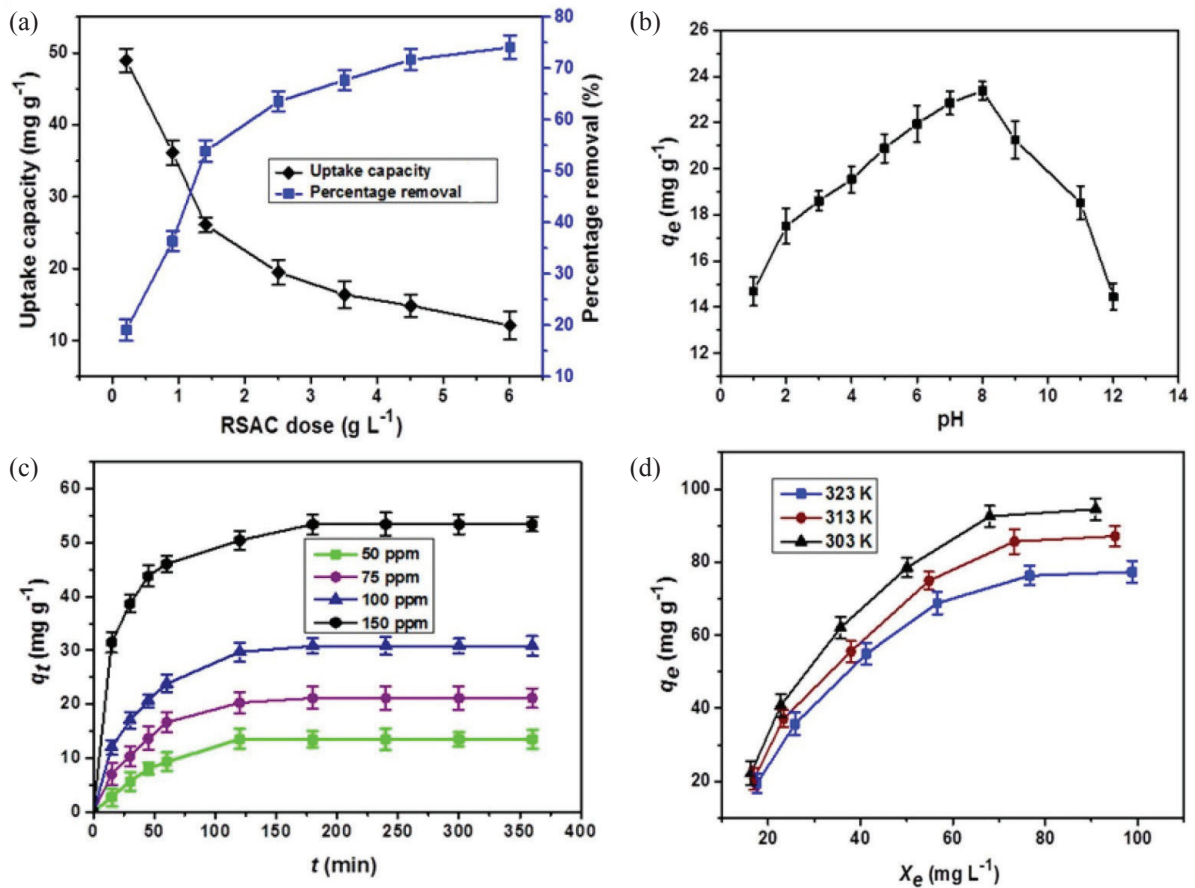


Fig. 5 – Effects of parameters for 2-CP adsorption onto RSAC (a) Effect of RSAC dose, (b) Effect of pH, (c) Effect of initial concentration and contact time, (d) Effect of temperature

tered at pH = 8. Hence, it can be concluded that the maximum adsorption of 2-CP was observed below its acid dissociation constant value.<sup>24</sup>

Since the highest adsorption occurred when the 2-CP was in its neutral form, it would not be appropriate to explain the pH effect behavior based on the point of zero charges of RSAC. Instead, this adsorption system can be satisfactorily explained with an electron donor-acceptor complex mechanism. In such mechanism, the aromatic ring of 2-CP acts as the electron acceptor, and the carbonyl oxygen on the RSAC surface acts as the electron donor. Due to this electron donor-acceptor complexation, an increase in the adsorption of 2-CP was registered up to the pH value of 8. After that, the adsorption efficiency reduced, since beyond the  $pK_a$  value, the 2-CP becomes anionic and is repelled by the negatively charged RSAC surface ( $pH > pH_{pzc}$ , the  $pH_{pzc}$  of RSAC was found to be 7.5), resulting in decreased adsorption.<sup>25</sup>

#### Effect of adsorbate-adsorbent contact time and 2-CP concentration variation

The optimal contact time for the highest adsorption of 2-CP onto RSAC was evaluated via experimental runs carried out with varying time periods in the range of 15 and 360 min at pH = 8 and adsorbent dose = 1.25 g L<sup>-1</sup> with an initial 2-CP concentration ( $X_0$ ) varying from 50–150 mg L<sup>-1</sup>. Fig. 5(c) depicts the trend of the 2-CP uptake ( $q_e$ , mg g<sup>-1</sup>) at different time intervals for the different initial concentrations of 2-CP.

From Fig. 5(c), it is evident that the extent of 2-CP adsorbed,  $q_e$  (mg g<sup>-1</sup>) followed an increasing trend with the increase in contact time for all the initial 2-CP concentrations. Moreover, the 2-CP adsorption was observed to follow an increasing pattern upon the increase in initial 2-CP concentration. Rapid adsorption of 2-CP onto RSAC was observed for an initial 70 min, and the rate gradually slowed down, and equilibrium was attained at about 125 min. The uptake capacity of 2-CP was obtained between ~9.48 to ~48.1 mg g<sup>-1</sup> for the corresponding increment of  $X_0$ , from 50 to 150 mg L<sup>-1</sup>. The fast adsorption rate for the initial 70 min period can be related to the vacancy of more adsorption sites at the initial stage, resulting in a higher concentration difference between the adsorbate in the solution and those on the adsorbent.<sup>26</sup> The reduction in concentration difference at later stages resulted in reduced uptake capacity rate and the onset of equilibrium. A similar trend for adsorption was seen for all the initial adsorbate concentrations. Following the equilibrium attainment timing, the adsorbate-adsorbent interaction duration of 125 min was considered the optimal contact time for the 2-CP-RSAC system.

#### Temperature effect on 2-CP adsorption

For studying the temperature effect on 2-CP adsorption, adsorptive runs were made at three different temperatures, 303, 313, and 323 K. The optimal values of other factors were RSAC dose, = 1.25 g L<sup>-1</sup>, pH = 8, while the 2-CP concentration was maintained at 100 mg L<sup>-1</sup> over all the temperatures. It was confirmed from Fig. 5(d) that the uptake capacity of RSAC for 2-CP decreased with the increase in temperature.

#### Adsorption kinetics study

Adsorption kinetics is crucial in investigating the optimal operating conditions for designing adsorption systems based on the uptake ability of adsorbent. Two reaction-based adsorption kinetics models, namely pseudo-first-order and pseudo-second-order, were chosen to fit the experimental data.<sup>27,28</sup> These models also provide information regarding the adsorbate uptake rate by adsorbent. In this study, the nonlinear regression analysis was carried out for the kinetics model fitting of experimental data. Moreover, Marquardt's percentage standard deviation error function was used for evaluating the appropriate model fit. The nonlinear model equations and the error function equation are represented by Eqs. 5–8.

$$q_t = (q_e - e^{-k_f t}) \quad (5)$$

$$q_t = \frac{k_s q_e^2 t}{1 + k_s q_e t} \quad (6)$$

The constant  $k_s$  is used for determining the initial rate of adsorption ' $h$ ' at time  $t \rightarrow 0$  using the following equation.  $h$  is in unit mg g<sup>-1</sup> min<sup>-1</sup>.

$$h = k_s q_e^2 \quad (7)$$

$$MPSD = 100 \sqrt{\frac{1}{n-p} \sum_{j=1}^n \left( \frac{(q_{e,exp} - q_{e,calc})}{q_{e,exp}} \right)^2} \quad (8)$$

where  $q_e$  = 2-CP uptake capacity of RSAC at equilibrium (mg g<sup>-1</sup>)

$q_t$  = 2-CP uptake capacity of RSAC at time,  $t$  (mg g<sup>-1</sup>)

$k_f$  = pseudo-first-order kinetic rate constant, (min<sup>-1</sup>)

$k_s$  = pseudo-second-order kinetic rate constant, (g mg<sup>-1</sup> min<sup>-1</sup>).

The pseudo-first- and second-order kinetic models were fitted with the experimental data by nonlinear regression technique. The highest-fit values of  $h$ ,  $k_s$ ,  $q_e$  and  $k_f$  along with the  $R^2$  for both the kinetics models for the 2-CP-RSAC adsorption process are presented in Table 2. The regression correlation coefficients ( $R^2$ ) were considered to evaluate

Table 2 – Kinetics modelling of experimental data for 2-CP-RSAC adsorption system

Concentration (mg L <sup>-1</sup> )	50	75	100	150
$q_{e,exp}$ (mg g <sup>-1</sup> )	14.5536	22.3972	31.8341	53.4611
Pseudo-first-order				
$q_{e,calc}$ (mg g <sup>-1</sup> )	14.7411	22.8415	31.8923	53.58
$k_f$ (min <sup>-1</sup> )	0.0192	0.0275	0.0369	0.0398
$R^2$	0.9854	0.9892	0.9912	0.9729
MPSD	14.52	9.83	11.79	10.66
Pseudo-second-order				
$q_{e,calc}$ (mg g <sup>-1</sup> )	18.2703	26.49	31.37	54.53
$h$ (mg g <sup>-1</sup> min <sup>-1</sup> )	0.2698	0.6528	2.3123	5.4551
$k_s$ (g mg <sup>-1</sup> min <sup>-1</sup> )	0.0023	0.019	0.0017	0.0106
$R^2$	0.9623	0.9701	0.9759	0.9865
MPSD	25.74	11.48	11.79	10.86

the best-fit model. Moreover, the calculated values of uptake capacity for pseudo-first-order kinetics models were close to those of experimental values. Referring to Table 2, it is evident that the experimental data are in good agreement with the pseudo-first-order kinetics model.

### Adsorption dynamics study

Adsorption dynamics studies were carried out to evaluate the mechanism of the 2-CP-RSAC adsorption. The research data were processed by Boyd kinetic model, as represented by Eq. 9.

$$B_t = -0.4977 - \ln(1 - F) \quad (9)$$

where  $F$  represents the fraction of 2-CP adsorbed at time interval  $t$  to that at equilibrium and can be expressed as  $F = q_t/q_e$ ,  $q_t$  is the quantity of 2-CP adsorbed in time  $t$ , and  $q_e$  is the equilibrium amount of adsorbed 2-CP.

The linear plot between  $B_t$  versus  $t$  presented in Fig. 6(a) confirms that 2-CP adsorption onto RSAC followed the film diffusion or external mass transport mechanism (since the linear plot did not pass through the origin) and was also the adsorption rate-limiting step.<sup>29</sup>

The effective diffusivity  $D_e$  (cm<sup>2</sup> s<sup>-1</sup>) was evaluated employing Eq. 10, using the  $B_t$  values obtained from Eq. 3<sup>30</sup>

$$B_t = \frac{\pi^2 D_e}{r^2} \quad (10)$$

where  $r$  represents the radius of adsorbent particles (assumed as spheres), and is estimated by sieve analysis.

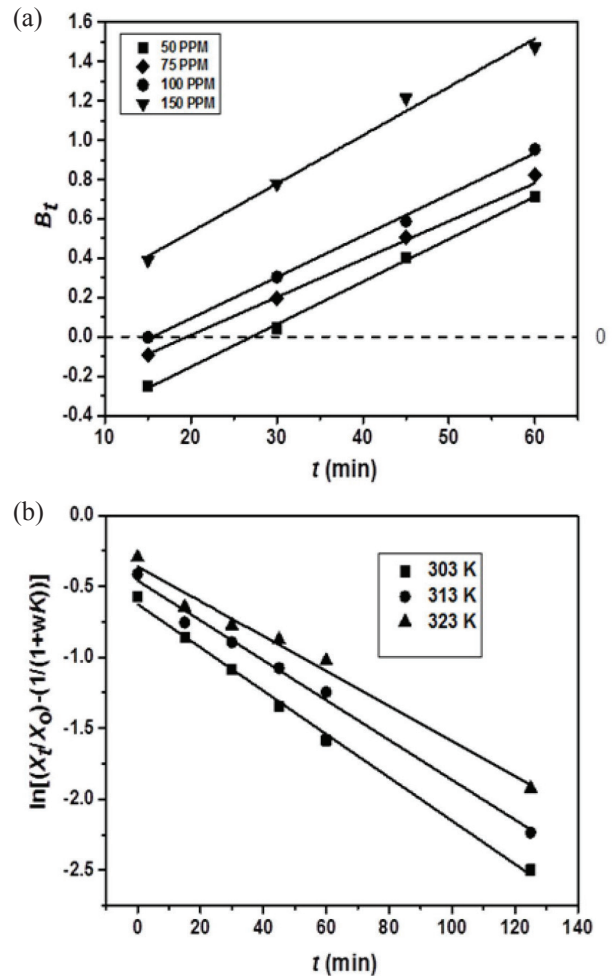


Fig. 6 – (a) Boyd plot for the abatement of 2-CP using RSAC, (b) External mass transfer plot for 2-CP-RSAC sorption system; with the parametric conditions as ( $X_0 = 50$ – $150$  mg L<sup>-1</sup>;  $t = 125$  min;  $w = 1.25$  g L<sup>-1</sup>;  $pH = 8$ )

With all the different adsorbent concentrations, the average value of  $D_e$  was  $4.16 \cdot 10^{-13}$  m<sup>2</sup> s<sup>-1</sup> for the 2-CP-RSAC adsorption system.

The adsorption mass transfer anomaly was investigated using Eq. 11

$$\ln\left[\frac{X_t}{X_0} - \frac{1}{1+wK}\right] = \ln\left[\frac{wK}{1+wK}\right] - \left[\frac{1+wK}{wK}\right] \beta_1 S_s t \quad (11)$$

where  $X_0$  (mg L<sup>-1</sup>) and  $X_t$  (mg L<sup>-1</sup>) are the 2-CP concentrations at the beginning and at time  $t$ , respectively;

$w$  (g) = weight of adsorbent

$K$  (L g<sup>-1</sup>) = Langmuir constant

$\beta_1$  (cm s<sup>-1</sup>) = coefficient of mass transfer

$S_s$  (L cm<sup>-1</sup>) = ratio of unit volume to the external surface of the adsorbent.

The linear graph of  $\ln[(X_t/X_0) - (1/(1+wK))]$  against  $t$  resulted in a straight line (Fig. 6(b)). The mass transfer coefficient value ( $\beta_1$ ) was evaluated

from the graph's intercept and slope of the resulting straight-line equation.

At initial adsorbate concentration of  $X_0 = 100 \text{ mg L}^{-1}$ , the mass transfer coefficient values ( $\beta_1$ ) values for the different temperatures such as 303, 313, and 323 K were found to be  $3.39 \cdot 10^{-7}$ ,  $2.84 \cdot 10^{-7}$ , and  $2.49 \cdot 10^{-7} \text{ cm s}^{-1}$ , respectively. The mass transfer coefficient values ( $\beta_1$ ) have signaled that the transfer of 2-CP ions from the bulk solution to the adsorbent surface was swift and provided affirmative evidence for RSAC as potent adsorbent for 2-CP abatement. Mondal *et al.* have reported a similar finding for adsorption mass transfer investigation study for orange G adsorption using hematite.<sup>31</sup>

### Adsorption equilibrium studies

Adsorption equilibrium provides necessary information about the relationship between the adsorbate concentration on the adsorbent surface and the bulk solution. This information obtained through adsorption equilibrium studies helps thoroughly understand the adsorption process mechanism, and assists effectively the design of adsorption systems.<sup>20,32</sup> In this study, four different isotherm models were used for fitting the experimental data over a temperature range of 303–333 K. Langmuir, Freundlich, and Temkin models were used among two-parameter equilibrium models. Whereas, the Redlich-Peterson model was the only model used among three-parameter models. Eqs. 12–14 represent the aforementioned equilibrium models, respectively. The non-linear form of each model was used for the study. Apart from the model fitting studies, error analysis study was also carried out using Marquardt's percent standard deviation (MPSD) error function represented by Eq. 8 used.

$$q_e = \frac{K_L X_e}{1 + K_L X_e} \quad (12)$$

$$q_e = K_F X_e^{1/n} \quad (13)$$

$$q_e = \frac{RT}{b_T} \ln K_T X_e \quad (14)$$

$$q_e = \frac{K_R X_e}{1 + a_R X_e^\beta} \quad (15)$$

where  $X_e$  = equilibrium concentration of 2-CP ( $\text{mg L}^{-1}$ )  
 $q_e$  = 2-CP uptake capacity of RSAC at equilibrium, ( $\text{mg g}^{-1}$ )

$q_m$  = complete monolayer uptake capacity of RSAC, ( $\text{mg g}^{-1}$ )

$K_L$  = Langmuir constant related to binding site affinities, ( $\text{L mg}^{-1}$ )

$K_F$  = Freundlich constant related to adsorption capacity, ( $\text{mg g}^{-1}$ )

$K_T$  = Temkin constant, ( $\text{L g}^{-1}$ )

$n$  = Freundlich constant related to the adsorption intensity, ( $\text{L mg}^{-1}$ )

$R$  = universal gas constant, ( $8.314 \cdot 10^{-3} \text{ kJ mol}^{-1} \text{ K}^{-1}$ )

$T$  = absolute temperature, (K)

$b_T$  = Temkin constant related to heat of adsorption, ( $\text{kJ mol}^{-1}$ )

$K_R$  = Redlich-Peterson constant, ( $\text{L g}^{-1}$ )

$a_R$  = Redlich-Peterson constant, ( $\text{L mg}^{-1}$ )

$\beta$  = Redlich-Peterson exponent and is a dimensionless entity, where the value is  $\leq 1$ . This equation becomes linear at a low surface coverage, i.e.,  $g = 0$ , and at  $g = 1$ , the equation converges to a Langmuir isotherm.

The adsorption equilibrium plot is presented in Fig. 7. Calculated values of all the constants involved with different isotherm models and their respective correlation coefficients ( $R^2$ ) at different temperatures are given in Table 3. Based on  $R^2$  values (higher for better fitting), the experimental data showed good agreement for fitting to the isotherm models in the order (of highest preferred to the lowest one) Langmuir >R-P>Temkin>Freundlich. As evident from Table 3, the Langmuir isotherm model was found to be the best fit model for experimental data. The maximum adsorption capacities as evaluated by this model were in the range of  $\sim 38$  to  $\sim 42 \text{ mg g}^{-1}$  for the aforementioned temperature range.

For the Temkin isotherm model, it was found that the bond energy of the ion-exchange process for all the temperatures fell in the bracket of 8–9  $\text{kJ mol}^{-1}$ , which confirmed the physisorption process, for which the criterion is that adsorption energies are  $< 40 \text{ kJ mol}^{-1}$ .<sup>33</sup> The variation in the values of  $B_T$  (8.54 to 8.71  $\text{kJ mol}^{-1}$ ) over a minimal range

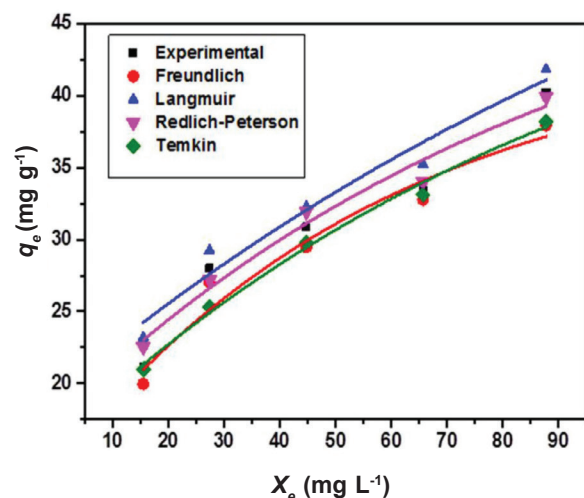


Fig. 7 – Adsorption equilibrium plot for 2-CP-RSAC adsorption system ( $X_0 = 50\text{--}150 \text{ mg L}^{-1}$ ;  $t = 125 \text{ min}$ ;  $w = 1.25 \text{ g L}^{-1}$ ;  $\text{pH} = 8$ ;  $T = 303 \text{ K}$ )

Table 3 – Isotherm modeling of experimental data for 2-CP-RSAC adsorption system

Freundlich						
Temp. (K)	$K_f$ (L mg <sup>-1</sup> )	1/n	$R^2$	MPSD		
303 K	7.6332	0.3117	0.9688	7.6123		
313 K	9.5392	0.3216	0.9673	12.2803		
323 K	4.5291	0.3802	0.9799	3.7338		
333 K	7.1363	0.3612	0.9581	4.0676		
Langmuir						
Temp. (K)	$q_m$ (mg g <sup>-1</sup> )	$K_L$ (L mg <sup>-1</sup> )	$R^2$	MPSD		
303 K	41.8321	0.0837	0.9991	2.8441		
313 K	39.2334	0.0685	0.9953	2.5463		
323 K	38.1573	0.0493	0.9978	1.4834		
333 K	39.4642	0.0546	0.9964	4.9569		
Temkin						
Temp. (K)	$K_T$ (L mg <sup>-1</sup> )	$B_T$ (kJ mol <sup>-1</sup> )	$R^2$	MPSD		
303 K	0.8321	8.5396	0.9946	4.7396		
313 K	0.6221	8.5678	0.9797	13.1833		
323 K	0.4672	8.6935	0.9843	2.5982		
333 K	0.3976	8.8261	0.9678	3.2428		
Redlich-Peterson						
Temp. (K)	$K_R$ (L g <sup>-1</sup> )	$\alpha_R$ (L mg <sup>-1</sup> )	$\beta$	$R^2$	MPSD	
303 K	1.941	0.0242	1.2419	0.9996	3.2445	
313 K	1.288	0.0347	1.6235	0.9942	11.5465	
323 K	15.164	1.8312	0.6743	0.9963	3.5167	
333 K	120.417	19.3006	0.6815	0.9873	4.0545	

Table 4 – Thermodynamic parameters for 2-CP abatement by RSAC ( $X_o = 50\text{--}150$  mg L<sup>-1</sup>;  $t = 125$  min; RSAC dose = 1.25 g L<sup>-1</sup>;  $pH_o = 8$ )

$X_o$ (mg L <sup>-1</sup> )	$\Delta H^\circ$ (kJ mol <sup>-1</sup> K <sup>-1</sup> )	$\Delta S^\circ$ (kJ mol <sup>-1</sup> K <sup>-1</sup> )	$\Delta G^\circ$ (kJ mol <sup>-1</sup> K <sup>-1</sup> )			
			303 K	313 K	323 K	333 K
50	-34.25	9.64	-16.21	-19.14	-20.19	-23.34
75	-13.33	12.68	-18.52	-18.98	-19.83	-20.06
100	-6.42	35.17	-17.36	-17.56	-18.36	-18.75
125	-4.23	62.39	-16.08	-17.23	-17.54	-17.97
150	-5.82	30.11	-17.29	-17.58	-17.93	-18.33

for this work indicated the involvement of chemisorption to a certain extent.<sup>34</sup> Moreover, it was observed that the adsorption intensity 'n' value was < 1 for all the temperatures in the Freundlich model, confirming that the 2-CP-RSAC adsorption was favorable.

### Thermodynamics of the 2-CP-RSAC adsorption process

The evaluation of thermodynamic parameters is crucial for investigating the nature, spontaneity, and feasibility of the adsorption process at the selected study temperature.<sup>35</sup>

The free energy of adsorption ( $\Delta G^\circ$ ) was evaluated by Eq. 16<sup>36</sup>

$$\Delta G^\circ = -RT \ln K \quad (16)$$

where,  $K$  (L mol<sup>-1</sup>) = equilibrium constant, derived from Langmuir isotherm model,

$R$  = universal gas constant, (8.314 J mol<sup>-1</sup> K<sup>-1</sup>)

$T$  = temperature (absolute).

The adsorption enthalpy change ( $\Delta H^\circ$ ) and entropy change ( $\Delta S^\circ$ ) were calculated by the Eqs. 17 and 18, respectively<sup>37</sup>

$$\Delta H^\circ = R \left( \frac{T_1 T_2}{T_1 - T_2} \right) \ln \frac{K_2}{K_1} \quad (17)$$

$$\Delta S^\circ = \frac{\Delta H^\circ - \Delta G^\circ}{T} \quad (18)$$

where,  $K_1$  and  $K_2$  are the equilibrium constants at corresponding temperatures of  $T_1$  and  $T_2$ , respectively.

The calculated values of  $\Delta H^\circ$ ,  $\Delta G^\circ$  and  $\Delta S^\circ$  using the previous equations are given in Table 4. The positive entropy change ( $\Delta S^\circ$ ) values confirmed an increase in randomness with the increase in adsorbate molecules on the adsorbent surface for the adsorption of 2-CP on RSAC. The negative values of  $\Delta G^\circ$  proved the spontaneity of the 2-CP adsorption process. According to Liu and Zhang,  $\Delta G^\circ$  values < -10 kJ mol<sup>-1</sup> suggests a multilayer adsorption process. The  $\Delta G^\circ$  values given in Table 4 thus confirmed the existence of multilayer adsorption.<sup>38,39</sup> The heat of adsorption ( $\Delta H^\circ$ ) values in the range of 0 and -20 kJ mol<sup>-1</sup> are very often considered as the indicator for physisorption.<sup>40</sup>

### Isosteric heat of adsorption

The Clausius-Clapeyron (C-C) equation was implemented for the evaluation of isosteric heat of adsorption ( $\Delta H_{st,a}$ ) at the condition of fixed surface fouling (considering only the equilibrium uptake capacity values of each experimental run).<sup>41</sup> The mathematical expression for evaluating isosteric heat of adsorption is represented by Eq. 19.

$$\frac{d \ln X_e}{dT} = \frac{-\Delta H_{st,a}}{RT^2} \quad (19)$$

The equilibrium concentration ( $X_e$ ) values were obtained from the adsorption equilibrium data at varying temperatures. The slope of the linear plot of

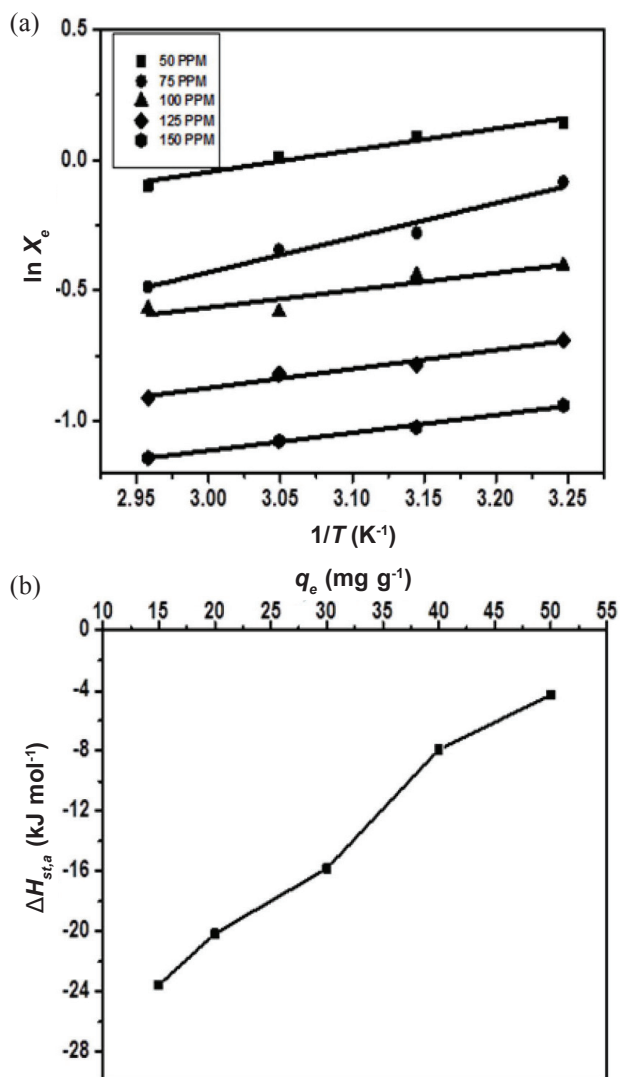


Fig. 8 – (a) Van't Hoff plot for the 2-CP-RSAC adsorption system ( $X_0 = 50\text{--}150$  mg L<sup>-1</sup>;  $t = 125$  min;  $w = 1.25$  g L<sup>-1</sup>;  $pH = 8$ ), (b) Isosteric heat of adsorption ( $\Delta H_{st,a}$ ) based on surface loading for 2-CP adsorption onto RSAC

$X_e$  against  $(1/T)$ , gives  $\Delta H_{st,a}$  value. Fig. 8(a) shows the corresponding isosters' respective equilibrium uptake capacities of 2-CP by RSAC at different adsorbate concentrations and time. Fig. 8(b), shows that  $\Delta H_{st,a}$  followed an increasing trend with the increase in  $q_e$  in equilibrium uptake capacity, thus confirming the heterogeneity of the RSAC surface.<sup>42</sup> The negativity of isosteric heat of adsorption values confirmed the exothermic nature of 2-CP adsorption.

#### Estimation of the thermodynamic parameter by statistical thermodynamics

Classical thermodynamics defines the overall energy and equilibrium conditions in an adsorption process. However, it fails to provide detailed information regarding the bulk properties of the adsorbate solution and adsorbent at microscopic levels. However, statistical thermodynamics enunciates this

information with ease.<sup>43</sup> Only the evaluation of various parameters involved in the statistical thermodynamics study is provided in this report. The detailed statistical thermodynamics study for the 2-CP-RSAC system has been communicated elsewhere for publication.

The value of  $\Delta G^\circ$  was also estimated using statistical thermodynamics, as explained by Wang and Jiang.<sup>44</sup>

$$\text{Since } \ln\left(\frac{1-\eta}{\eta}\right) = \frac{\Delta G^\circ}{\gamma} - \frac{RT \ln X}{\gamma} \quad (20)$$

where  $\gamma$  is the distribution modulus, and  $\eta$  is the fraction of 2-chlorophenol adsorbed from the bulk solution.

The plot of  $\ln[(1-\eta)/\eta]$  against  $\ln X$  over different temperatures studied for 2-CP and RSAC system. The value of  $\gamma$  was estimated from the slope of the plot, and the  $\Delta G^\circ$  values were determined from the intercept of the straight-line equation. According to eq. values of  $\Delta S^\circ$  and  $\Delta H^\circ$  were determined from the slope and intercept of  $\Delta G^\circ$  versus  $T$  plot (not reported here).

$$\Delta G^\circ = \Delta H^\circ - T\Delta S^\circ \quad (21)$$

The values of  $\Delta G^\circ$ ,  $\Delta H^\circ$  and  $\Delta S^\circ$  for different systems are shown in Table 5. The results given in Table 5 satisfactorily describe the spontaneity and exothermic nature of the adsorption system with the micromolecular viewpoint. The results of the classical thermodynamics modeling (Table 4) were found to be in accordance with those of statistical thermodynamics modeling, indicating that the thermodynamic modeling of the 2-CP-RSAC adsorption system can be performed with any of these two approaches.

#### RSAC regeneration

The results confirmed that the RSAC uptake capacity was restored up to 90 % after regeneration for four consecutive cycles. The usage of NaOH in the regeneration process resulted in the formation of easily separable sodium salts of the 2-CP on RSAC, thereby making the regeneration operation easier.<sup>45</sup> Fig. 9 represents the RSAC regeneration efficiency plot.

#### Mechanism of 2-CP adsorption onto RSAC

The adsorption mechanism depends on the adsorbent's surface properties and the chemistry of adsorbate. There are several possible mechanisms for the adsorption of 2-CP (aromatic organic pollutant) onto carbonaceous adsorbents, such as;  $\pi$ - $\pi$  bond interaction, hydrogen bonding (H-bonding), electron donor-acceptor complexation, and electro-

Table 5 – Thermodynamic parameters using classical statistical physics for 2-CP sorption onto RSAC ( $X_o = 50\text{--}150\text{ mg L}^{-1}$ ;  $t = 125\text{ min}$ ; RSAC dose =  $1.25\text{ g L}^{-1}$ ;  $pH_o = 8$ )

$X_o$ (mg L <sup>-1</sup> )	$\Delta H^\circ$ (kJ mol <sup>-1</sup> K <sup>-1</sup> )	$\Delta S^\circ$ (kJ mol <sup>-1</sup> K <sup>-1</sup> )	$\Delta G^\circ$ (kJ mol <sup>-1</sup> K <sup>-1</sup> )			
			303 K	313 K	323 K	333 K
50	-33.79	8.35	-17.21	-17.35	-17.82	-20.49
75	-12.75	12.17	-16.96	-17.93	-18.67	-19.26
100	-5.86	33.17	-16.28	-16.50	-17.77	-18.41
125	-3.59	63.15	-17.10	-17.54	-17.86	-18.34
150	-5.34	30.83	-16.89	-17.19	-17.38	-17.78

Table 6 – Comparative study with other methods

Method	Intricate details	Performance	Reference
Photocatalytic degradation	*InVO <sub>4</sub> /TiO <sub>2</sub> catalyst + visible light	50.5 % degradation achieved	47
Low-pressure reverse osmosis	TW30-1812-100 low-pressure membrane	79 % rejection was observed	48
Solvent mediated ozonolysis	The solvent used was decamethylcyclopentasiloxane	95 % degradation was achieved in ~30 sec	49
Biocatalyst assisted ultrasonication	Horse radish peroxidase as the biocatalyst	~100 % degradation was achieved in 30 min	50
Activated carbon mediated adsorption	Rice straw activated carbon activated with ZnCl <sub>2</sub>	74 % removal was achieved	This study

\*In = Indium, V = Vanadium, Ti = Titanium. Actual comparison among the methods is impossible since each of the methods listed above has its own set of experimental parameters.

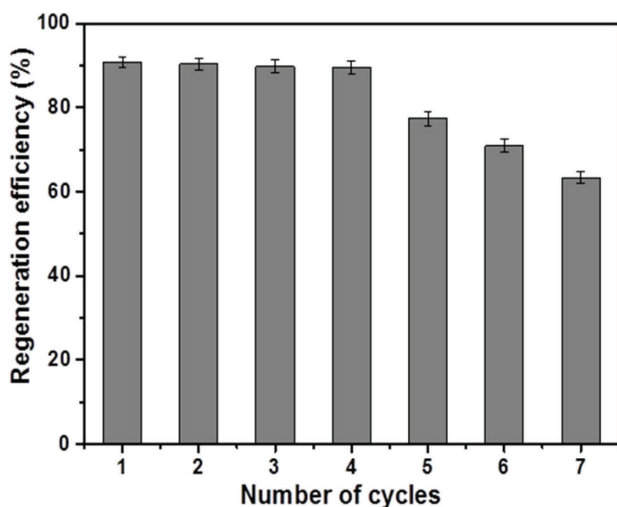


Fig. 9 – Regeneration efficiency of RSAC

static interaction. However, from the experimental study of this 2-CP-RSAC adsorption system, the underlying mechanisms can pertain to the hydrogen bonding and electron donor-acceptor complexation concepts.<sup>24,46</sup>

The H-bonding was established between the hydrogen atom of the hydroxyl group of 2-CP and the more electronegative atoms like oxygen and nitrogen present on the surface of RSAC. The schematic representation of the H-bonding concept is presented in Fig. 10(a). The electron donor-acceptor complexation concept involves two entities, such as

the oxygen atom of the carbonyl group on the RSAC surface and the aromatic ring of 2-CP, which act as the electron donor and acceptor respectively, as shown in Fig. 10(b).

The comparative performances of various methods used for 2-CP removal are represented in Table 6, and adsorbent performance comparison for 2-CP removal is provided in Table 7. From Table 6, it can be concluded that adsorption is a robust method for removing 2-CP from aqueous solutions. Table 7 has provided evidence for confirming that the RSAC is a cheap yet effective adsorbent for the adsorptive removal of 2-CP.

## Conclusions

The characterization studies performed on RSAC have revealed its characteristic features. Proximate, ultimate, and EDX analyses confirmed the presence of higher percentages of carbon as much as 56.33, 55.48, and 66.38 percent, respectively. The point of zero charge study revealed that the RSAC surface is neutral at pH 7.5. BET and pore size analyses showed that the RSAC had a surface area of  $239\text{ m}^2\text{ g}^{-1}$ , cumulative pore volume of  $0.186\text{ cm}^3\text{ g}^{-1}$ , and pore width of  $25.62\text{ \AA}$ , respectively. The SEM analysis revealed mesoporous structure formation due to the influence of chemical impregnation and high-temperature carbonization.

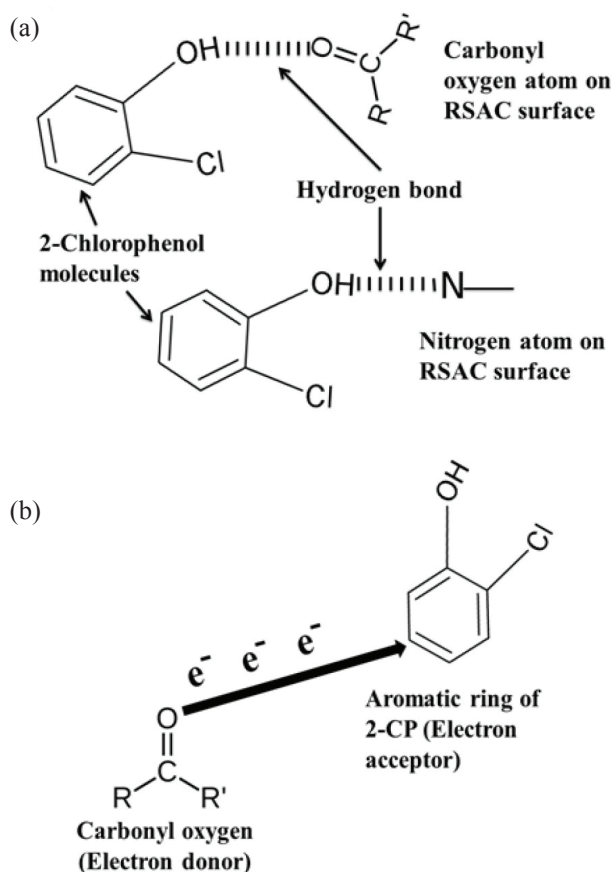


Fig. 10 – Schematics for the mechanism of 2-CP adsorption onto RSAC (a) H-bonding (b) Electron donor-acceptor complex formation

FTIR analysis confirmed the presence of hydroxyl, sulfinyl, and carbonyl functional groups on the surface of RSAC.

The experimental results revealed the efficacy of RSAC for the abatement of 2-CP from water and wastewater. The optimal conditions for the parameters affecting adsorption of 2-CP onto RSAC were evaluated. The optimal values for parameters RSAC dose, pH, contact time, and temperatures were found to be 1.25 g L<sup>-1</sup>, 8, 125 min, and 303 K, respectively. Furthermore, it was observed that the adsorption capacity started to decline with the increase in the system temperature. The adsorption kinetics data were found to follow the pseudo-first-order kinetics model. Adsorption equilibrium data for the 2-CP-RSAC system were best fitted with Langmuir and Redlich-Peterson isotherm models suggesting the existence of chemical and physical adsorption modes. The Boyd plot confirmed that the external mass transfer was the slowest step in this adsorption study. Thermodynamic studies demonstrated that the 2-CP-RSAC adsorption system was spontaneous and exothermic by nature. The regeneration studies of RSAC revealed that the regenerability of RSAC remained intact for four consecutive cycles of regeneration.

Table 7 – Comparative study of the 2-CP uptake capacity by various adsorbents

Adsorbent used	Adsorption capacity (mg g <sup>-1</sup> )	References
Rice-straw-based carbon	14.2	51
Cross-linked algae <i>Macroscystis integrifolia</i> Bory	34.614	52
XAD-4	41.14	53
CMSt/DVB	20.57	53
Neem seed activated carbon	41	15
ZnCl <sub>2</sub> impregnated rice straw activated carbon	45.34	this study

## References

- Zada, A., Khan, M., Khan, M. A., Khan, Q., Habibi-Yangjeh, A., Dang, A., Maqbool, M., Review on the hazardous applications and photodegradation mechanisms of chlorophenols over different photocatalysts, *Environ. Res.* **195** (2021) 110742. doi: <https://doi.org/10.1016/j.envres.2021.110742>
- Huong, P.-T., Lee, B.-K., Kim, J., Improved removal of 2-chlorophenol by a synthesized Cu-nano zeolite, *Process Saf. Environ. Prot.* **100** (2016) 272. doi: <https://doi.org/10.1016/j.psep.2016.02.002>
- Pera-Titus, M., García-Molina, V., Baños, M. A., Giménez, J., Esplugas, S., Degradation of chlorophenols by means of advanced oxidation processes: A general review, *Appl. Catal., B.* **47** (2004) 219. doi: <https://doi.org/10.1016/j.apcatb.2003.09.010>
- Shen, T., Wang, P., Hu, L., Hu, Q., Wang, X., Zhang, G., Adsorption of 4-chlorophenol by wheat straw biochar and its regeneration with persulfate under microwave irradiation, *J. Environ. Chem. Eng.* **9** (2021) 105353. doi: <https://doi.org/10.1016/j.jece.2021.105353>
- Barakat, M. A., Kumar, R., Eniola, J. O., Adsorption and photocatalytic scavenging of 2-chlorophenol using carbon nitride-titania nanotubes based nanocomposite: Experimental data, kinetics and mechanism, *Data Brief.* **34** (2021) 106664. doi: <https://doi.org/10.1016/j.dib.2020.106664>
- Enoyh, C. E., Isiuku, B. O., Competitive biosorption and phytotoxicity of chlorophenols in aqueous solution to *Canna indica* L., *Current Res. Green and Sust. Chem.* **4** (2021) 100094. doi: <https://doi.org/10.1016/j.crgsc.2021.100094>
- Liu, T., Cui, K., Chen, Y., Li, C., Cui, M., Yao, H., Chen, Y., Wang, S., Removal of chlorophenols in the aquatic environment by activation of peroxymonosulfate with nMnOx@Biochar hybrid composites: Performance and mechanism, *Chemosphere* **283** (2021) 131188. doi: <https://doi.org/10.1016/j.chemosphere.2021.131188>
- Kusmierek, K., Kicinski, W., Norek, M., Polanski, M., Budner, B., Oxidative and adsorptive removal of chlorophenols over Fe-, N- and S-multi-doped carbon xerogels, *J. Environ. Chem. Eng.* **9** (2021) 105568. doi: <https://doi.org/10.1016/j.jece.2021.105568>
- Garba, Z., Zhou, W., Lawan, I., Xiao, W., Zhang, M., Wang, L., Chen, L., Yuan, Z., An overview of chlorophenols as contaminants and their removal from wastewater by adsorption: A review, *J. Environ. Manage.* **241** (2019) 59. doi: <https://doi.org/10.1016/j.jenvman.2019.04.004>

10. *Kozyatnyk, I., Yacout, D. M. M., Caneghem, J. V., Jansson, S.*, Comparative environmental assessment of end-of-life carbonaceous water treatment adsorbents, *Bioresour. Technol.* **302** (2020) 122866.  
doi: <https://doi.org/10.1016/j.biortech.2020.122866>
11. *Zhang, T., Yang, Y., Li, X., Jiang, Y., Fan, X., Du, P., Li, H., Wang, N., Zhou, Z.*, Adsorption characteristics of chloramphenicol onto powdered activated carbon and its desorption performance by ultrasound, *Environ. Technol.* **42** (2021) 571.  
doi: <https://doi.org/10.1080/09593330.2019.1637464>
12. *Liang, Q., Liu, Y., Chen, M., Ma, L., Yang, B., Li, L., Liu, Q.*, Optimized preparation of activated carbon from coconut shell and municipal sludge, *Mater. Chem. Phys.* **241** (2020) 122327.  
doi: <https://doi.org/10.1016/j.matchemphys.2019.122327>
13. *Egbosiuba, T. C., Abdulkareem, A. S., Kovo, A. S., Afolabi, E. A., Tijani, J. O., Auta, M., Roos, W. D.*, Ultrasonic enhanced adsorption of methylene blue onto the optimized surface area of activated carbon: Adsorption isotherm, kinetics and thermodynamics, *Chem. Eng. Res. Des.* **153** (2020) 315.  
doi: <https://doi.org/10.1016/j.cherd.2019.10.016>
14. *Mahmood, T., Saddique, M. T., Naeem, A., Westerhoff, P., Mustafa, S., Alum, A.*, Comparison of different methods for the point of zero charge determination of NiO, *Ind. Eng. Chem. Res.* **50** (2011) 10017.  
doi: <https://doi.org/10.1021/ie200271d>
15. *Mahapatra, M. K., Kumar, A.*, Taguchi optimization studies for abatement of 2-chlorophenol using neem seed activated carbon, *Chem. Eng. Technol.* **45** (2022) 1.  
doi: <https://doi.org/10.1002/ceat.202100427>
16. *Juang, R.-S., Yei, Y.-C., Liao, C.-S., Lin, K.-S., Lu, H.-C., Wang, S.-F., Sun, A.-C.*, Synthesis of magnetic Fe<sub>3</sub>O<sub>4</sub>/activated carbon nanocomposites with high surface area as recoverable adsorbents, *J. Taiwan Inst. Chem. Eng.* **90** (2018) 51.  
doi: <https://doi.org/10.1016/j.jtice.2017.12.005>
17. *Machado, L. M. M., Lütkke, S. F., Perondi, D., Godinho, M., Oliveira, M. L. S., Collazzo, G. C., Dotto, G. L.*, Treatment of effluents containing 2-chlorophenol by adsorption onto chemically and physically activated biochars, *J. Environ. Chem. Eng.* **8** (2020) 104473.  
doi: <https://doi.org/10.1016/j.jece.2020.104473>
18. *Ji, Y., Zhong, H., Chen, P., Xu, X., Wang, Y., Wang, H., Liu, H.*, Single and simultaneous adsorption of methyl orange and p-chlorophenol on organo-vermiculites modified by an asymmetric gemini surfactant, *Colloids Surf., A.* **580** (2019) 123740.  
doi: <https://doi.org/10.1016/j.colsurfa.2019.123740>
19. *Li, X., Chen, S., Fan, X., Quan, X., Tan, F., Zhang, Y., Gao, J.*, Adsorption of ciprofloxacin, bisphenol and 2-chlorophenol on electrospun carbon nanofibers: In comparison with powder activated carbon, *J. Colloid Interface Sci.* **447** (2015) 120.  
doi: <https://doi.org/10.1016/j.jcis.2015.01.042>
20. *Qaid, F. A., Azzahari, A. D., Yahaya, A. H., Yahya, R. B.*, Adsorption of 4-chlorophenol from wastewater-based activated carbon prepared from *Jatropha* seed husks, *Desalin. Water Treat.* **57** (2016) 1.  
doi: <https://doi.org/10.1080/19443994.2015.1035497>
21. *Jabeen, A., Bhatti, H. N., Noreen, S., Gaffar, A.*, Adsorptive removal of 2, 4, 6-trichloro-phenol from wastewater by mango seed shell and its magnetic composites: Batch and column study, *Int. J. Environ. Anal. Chem.* **101** (2021) 1.  
doi: <https://doi.org/10.1080/03067319.2021.1941916>
22. *Liu, C., You, J., Hu, R., Jiang, W., Duan, Y., Li, J., Li, Z., Zhu, R., Li, Y., Liu, Z., Wang, K., Chen, C.*, Removal of bisphenol A and 2, 4-dichlorophenol from lake water using a flower-like covalent organic framework, *Anal. Lett.* **54** (2021) 347.  
doi: <https://doi.org/10.1080/00032719.2020.1764969>
23. *Banat, F. A., Al-Bashir, B., Al-Asheh, S., Hayajneh, O.*, Adsorption of phenol by bentonite, *Environ. Pollut.* **107** (2000) 391.  
doi: [https://doi.org/10.1016/S0269-7491\(99\)00173-6](https://doi.org/10.1016/S0269-7491(99)00173-6)
24. *Wang, X., Li, H., Huang, J.*, Adsorption of p-chlorophenol on three amino-modified hyper-cross-linked resins, *J. Colloid Interface Sci.* **505** (2017) 585.  
doi: <https://doi.org/10.1016/j.jcis.2017.06.053>
25. *Adane, B., Siraj, K., Meka, N.*, Kinetic, equilibrium and thermodynamic study of 2-chlorophenol adsorption onto *Ricinus communis* pericarp activated carbon from aqueous solutions, *Green Chem. Lett. Rev.* **8** (2015) 1.  
doi: <https://doi.org/10.1080/17518253.2015.1065348>
26. *Tan, I. A. W., Ahmad, A. L., Hameed, B. H.*, Adsorption isotherms, kinetics, thermodynamics and desorption studies of 2,4,6-trichlorophenol on oil palm empty fruit bunch-based activated carbon, *J. Hazard. Mater.* **164** (2009) 473.  
doi: <https://doi.org/10.1016/j.jhazmat.2008.08.025>
27. *López-Luna, J., Ramírez-Montes, L. E., Martínez-Vargas, S., Martínez, A. I., Mijangos-Ricardez, O. F., González-Chávez, M., Carrillo-González, R., Solís-Domínguez, F. A., Cuevas-Díaz, M., Vázquez-Hipólito, V.*, Linear and nonlinear kinetic and isotherm adsorption models for arsenic removal by manganese ferrite nanoparticles, *SN Appl. Sci.* **950** (2019) 1.  
doi: <https://doi.org/10.1007/s42452-019-0977-3>
28. *Hashem, A., Al-Anwar, A., Nagy, N. M., Hussein, D. M., Eisa, S.*, Isotherms and kinetic studies on adsorption of Hg(II) ions onto *Ziziphys spina-christi* L. from aqueous solutions, *Green Process. Synth.* **5** (2016) 213.  
doi: <https://doi.org/10.1515/gps-2015-0103>
29. *Dotto, G., McKay, G.*, Current scenario and challenges in adsorption for water treatment, *J. Environ. Chem. Eng.* **8** (2020) 103988.  
doi: <https://doi.org/10.1016/j.jece.2020.103988>
30. *Kumar, K. V., Ramamurthi, V., Sivanesan, S.*, Biosorption of malachite green, a cationic dye onto *Pithophora* sp., fresh water algae, *Dyes. Pigm.* **69** (2006) 102.  
doi: <https://doi.org/10.1016/j.dyepig.2005.02.005>
31. *Mondal, M. K., Singh, S., Umareddy, M., Dasgupta, B.*, Removal of Orange G from aqueous solution by hematite: Isotherm and mass transfer studies, *Korean J. Chem. Eng.* **27** (2010) 1811.  
doi: <https://doi.org/10.1007/s11814-010-0301-9>
32. *Ayawei, N., Ebelegi, A. N., Wankasi, D.*, Modelling and interpretation of adsorption isotherms, *J. Chem.* **2017** (2017) 3039817.  
doi: <https://doi.org/10.1155/2017/3039817>
33. *Mane, V. S., Mall, I. D., Srivastava, V. C.*, Use of bagasse fly ash as an adsorbent for the removal of brilliant green dye from aqueous solution, *Dyes. Pigm.* **73** (2007) 269.  
doi: <https://doi.org/10.1016/j.dyepig.2005.12.006>
34. *Hu, X.-J., Wang, J.-S., Liu, Y.-G., Li, X., Zeng, G.-M., Bao, Z.-L., Zeng, X.-X., Chen, A.-W., Long, F.*, Adsorption of chromium (VI) by ethylenediamine modified cross-linked magnetic chitosan resin: Isotherms, kinetics and thermodynamics, *J. Hazard. Mater.* **185** (2011) 306.  
doi: <https://doi.org/10.1016/j.jhazmat.2010.09.034>
35. *Elayadi, F., Boumya, W., Achak, M., Chhiti, Y., Alaoui, F.-E., Barka, N., Adlouni, C. E.*, Experimental and modeling studies of the removal of phenolic compounds from olive mill wastewater by adsorption on sugarcane bagasse, *Env. Challenge.* **4** (2021) 100184.  
doi: <https://doi.org/10.1016/j.envc.2021.100184>

36. Lu, M., Cheng, Y., Pan, S., Wei, G., Batch adsorption of p-nitrophenol by ZSM-11: Equilibrium, kinetic, and thermodynamic studies, *Desalination Water Treat.* **57** (2016) 3029. doi: <https://doi.org/10.1080/19443994.2014.983986>
37. Tan, I. A. W., Ahmad, A. L., Hameed, B. H., Adsorption, isotherm, kinetics, thermodynamics and desorption studies of 2,4,6-trichlorophenol on oil palm empty fruit bunch-based activated carbon, *J. Hazard. Mater.* **164** (2009) 473. doi: <https://doi.org/10.1016/j.jhazmat.2008.08.025>
38. Garba, Z., Rahim, A., Evaluation of optimal activated carbon from an agricultural waste for the removal of para-chlorophenol and 2, 4-dichlorophenol, *Process Saf. Environ. Prot.* **102** (2016) 54. doi: <https://doi.org/10.1016/j.psep.2016.02.006>
39. Liu, X., Zhang, L., Removal of phosphate anions using the modified chitosan beads: Adsorption kinetic, isotherm and mechanism studies, *Powder Technol.* **277** (2015) 112. doi: <https://doi.org/10.1016/j.powtec.2015.02.055>
40. Singh, S., Srivastava, V., Mall, I., Fixed-bed study for adsorptive removal of furfural by activated carbon, *Colloids Surf. A Physicochem. Eng. Asp.* **332** (2009) 50. doi: <https://doi.org/10.1016/j.colsurfa.2008.08.025>
41. Chen, Y., Tang, J., Wang, S., Zhang, L., Sun, W., Bimetallic coordination polymer for highly selective removal of Pb(II): Activation energy, isosteric heat of adsorption and adsorption mechanism, *Chem. Eng. J.* **425** (2021) 131474. <https://doi.org/10.1016/j.cej.2021.131474>
42. Cimino, R. T., Kowalczyk, P., Ravikovitch, P. I., Neimark, A. V., Determination of isosteric heat of adsorption by quenched solid density functional theory, *Langmuir.* **33** (2017) 1769. doi: <https://doi.org/10.1021/acs.langmuir.6b04119>
43. Knopf, D. A., Ammann, M., Technical note: Classical and statistical thermodynamic treatment of adsorption and desorption kinetics and rates, *Atmos. Chem. Phys.* **21** (2021) 15725. doi: <https://doi.org/10.5194/acp-21-15725-2021>
44. Wang, H.-L., Jiang, W.-F., Adsorption of dinitro butyl phenol (DNBP) from aqueous solutions by fly ash, *Ind. Eng. Chem. Res.* **46** (2007) 5405. doi: <https://doi.org/10.1021/ie070332d>
45. Jain, R., Sikarwar, S., Adsorption and desorption studies of Congo red using low-cost adsorbent: Activated de-oiled mustard, *Desalin. Water Treat.* **52** (2014) 7400. doi: <https://doi.org/10.1080/19443994.2013.837004>
46. Soltani, T., Lee, B.-K., Mechanism of highly efficient adsorption of 2-chlorophenol onto ultrasonic graphene materials: Comparison and equilibrium, *J. Colloid Interface Sci.* **481** (2016) 168. doi: <https://doi.org/10.1016/j.jcis.2016.07.049>
47. Rashid, J., Barakat, M. A., Pettit, S. L., Kuhn, K. N., InVO<sub>4</sub>/TiO<sub>2</sub> composite for visible-light photocatalytic degradation of 2-chlorophenol in wastewater, *Environ. Technol.* **35** (2014) 2153. doi: <https://doi.org/10.1080/09593330.2014.895051>
48. Kargari, A., Khazaali, F., Effect of operating parameters on 2-chlorophenol removal from wastewaters by a low-pressure reverse osmosis system, *Desalin. Water Treat.* **55** (2015) 114. doi: <https://doi.org/10.1080/19443994.2014.913993>
49. Ward, D. B., Tizaoui, C., Slater, M. J., Extraction and destruction of organics in wastewater using ozone-loaded solvent, *Ozone: Sci. Eng.* **26** (2004) 475. doi: <https://doi.org/10.1080/01919510490507801>
50. Entezari, M. H., Mostafai, M., Sarafraz-yazdi, A., A combination of ultrasound and a bio-catalyst: removal of 2-chlorophenol from aqueous solution, *Ultrason. Sonochem.* **13** (2006) 37. doi: <https://doi.org/10.1016/j.ultsonch.2004.11.002>
51. Namasivayam, C., Kavitha, D., Adsorptive removal of 2-chlorophenol by low-cost coir pith carbon, *J. Hazard. Mater. B.* **98** (2003) 257. doi: [https://doi.org/10.1016/S0304-3894\(03\)00006-2](https://doi.org/10.1016/S0304-3894(03)00006-2)
52. Navarro, A. E., Cuizano, N. A., Portales, R. F., Llanos, B. P., Adsorptive removal of 2-nitrophenol and 2-chlorophenol by cross-linked algae from aqueous solutions, *Sep. Sci. Technol.* **43** (2008) 3183. doi: <https://doi.org/10.1080/01496390802221642>
53. Simsek, E. B., Aytas, B., Duranoglu, D., Beker, U., Trochimczuk, A. W., A comparative study of 2-chlorophenol, 2,4-dichlorophenol, and 2,4,6-trichlorophenol adsorption onto polymeric, commercial, and carbonaceous adsorbents, *Desalin. Water Treat.* **57** (2015) 9940. doi: <https://doi.org/10.1080/19443994.2015.1033478>